NAVAL POSTGRADUATE SCHOOL

MONTEREY, CALIFORNIA

THESIS

A MODEL OF BORDER PATROL TO SUPPORT OPTIMAL OPERATION OF BORDER SURVEILLANCE SENSORS

by

Dolev Cfir

December 2005

Thesis Advisor:	Roberto Szechman
Second Reader:	Moshe Kress

Approved for public release; distribution is unlimited.

THIS PAGE INTENTIONALLY LEFT BLANK

REPORT DOCUMENTATION PAGE			Form Approved OMB No. 0704-0188
Public reporting burden for this collection of information is estimated to average 1 hour per response, including the time for reviewing instruction, searching existing data sources, gathering and maintaining the data needed, and completing and reviewing the collection of information. Send comments regarding this burden estimate or any other aspect of this collection of information, including suggestions for reducing this burden, to Washington headquarters Services, Directorate for Information Operations and Reports, 1215 Jefferson Davis Highway, Suite 1204, Arlington, VA 22202-4302, and to the Office of Management and Budget, Paperwork Reduction Project (0704-0188) Washington DC 20503.			
1. AGENCY USE ONLY ***(Leave blank)***	**2. REPORT DATE** December 2005	**3. REPORT TYPE AND DATES COVERED** Master's Thesis	
4. TITLE AND SUBTITLE: A Model of Border Patrol to Support Optimal Operation of Border Surveillance Sensors			**5. FUNDING NUMBERS**
6. AUTHOR(S) Dolev Cfir			
7. PERFORMING ORGANIZATION NAME(S) AND ADDRESS(ES) Naval Postgraduate School Monterey, CA 93943-5000			**8. PERFORMING ORGANIZATION REPORT NUMBER**
9. SPONSORING /MONITORING AGENCY NAME(S) AND ADDRESS(ES) N/A			**10. SPONSORING/MONITORING AGENCY REPORT NUMBER**
11. SUPPLEMENTARY NOTES The views expressed in this thesis are those of the author and do not reflect the official policy or position of the Department of Defense or the U.S. Government.			
12a. DISTRIBUTION / AVAILABILITY STATEMENT Approved for public release; distribution is unlimited.			**12b. DISTRIBUTION CODE**

13. ABSTRACT (maximum 200 words)

Borders are monitored by a variety of moving and stationary sensors, e.g., patrol agents, video cameras, ground sensors, UAVs, etc. This paper introduces a model for a moving sensor that patrols a perimeter that is infiltrated by malevolent agents (targets). Targets arrive according to a Poisson process along the perimeter with a certain distribution of arrival location, and disappear (renege) a random amount of time after their arrival. The measures of effectiveness (MOEs) presented in this paper are the target detection rate and the time elapsed from target arrival to its detection (waiting time). We study two types of sensor trajectories that are periodic and with constant speed:

1. The sensor moves from a starting point to a certain location and then leaps instantaneously back to the starting point.
2. The sensor moves back and forth between two points.

The controlled parameters (decision variables) are the beginning and end points of the patrolled sector. Properties of these trajectories are demonstrated in great generality. The results give decision makers a powerful tool for optimally deploying and operating a variety of sensors in an area of interest.

14. SUBJECT TERMS Border Patrol, Optimal Trajectory, Target Detection, Moving Sensor, Unmanned Aerial Vehicle, Detection Rate, Stochastic Model, Border Surveillance, Immigration Control			**15. NUMBER OF PAGES** 47
			16. PRICE CODE
17. SECURITY CLASSIFICATION OF REPORT Unclassified	**18. SECURITY CLASSIFICATION OF THIS PAGE** Unclassified	**19. SECURITY CLASSIFICATION OF ABSTRACT** Unclassified	**20. LIMITATION OF ABSTRACT** UL

NSN 7540-01-280-5500 Standard Form 298 (Rev. 2-89)
Prescribed by ANSI Std. 239-18

THIS PAGE INTENTIONALLY LEFT BLANK

Approved for public release; distribution is unlimited.

A MODEL OF BORDER PATROL TO SUPPORT OPTIMAL OPERATION OF BORDER SURVEILLANCE SENSORS

Dolev Cfir
Captain, Israeli Defense Force
B.S., Ben Gurion University, Israel, 1999

Submitted in partial fulfillment of the
requirements for the degree of

MASTER OF SCIENCE IN OPERATIONS RESEARCH

from the

NAVAL POSTGRADUATE SCHOOL
December 2005

Author: Dolev Cfir

Approved by: Roberto Szechman
Thesis Advisor

Moshe Kress
Second Reader

James N. Eagle
Chairman, Department of Operations Research

THIS PAGE INTENTIONALLY LEFT BLANK

ABSTRACT

Borders are monitored by a variety of moving and stationary sensors, e.g., patrol agents, video cameras, ground sensors, UAVs, etc. This paper introduces a model for a moving sensor that patrols a perimeter that is infiltrated by malevolent agents (targets). Targets arrive according to a Poisson process along the perimeter with a certain distribution of arrival location, and disappear (renege) a random amount of time after their arrival. The measures of effectiveness (MOEs) presented in this paper are the target detection rate and the time elapsed from target arrival to its detection (waiting time). We study two types of sensor trajectories that are periodic and maintain constant speed:

1. The sensor moves from a starting point to a certain location and then leaps instantaneously back to the starting point.
2. The sensor moves back and forth between two points.

The controlled parameters (decision variables) are the beginning and end points of the patrolled sector. Properties of these trajectories are demonstrated in great generality. The results give decision makers a powerful tool for optimally deploying and operating a variety of sensors in an area of interest.

THIS PAGE INTENTIONALLY LEFT BLANK

TABLE OF CONTENTS

I. INTRODUCTION 1
   A. GENERAL 1
   B. PREVIOUS WORK 2
   C. THE MODEL FRAMEWORK 2
II. THE LTO TRAJECTORY 7
   A. THE RATE OF DETECTION AS A FUNCTION OF SECTOR LENGTH 7
   B. OPTIMALITY CONDITIONS 12
   C. CHANGES IN VELOCITY 15
   D. SCANNING OF DISJOINT SECTORS 15
III. THE BACK AND FORTH TRAJECTORY 17
   A. RATE OF DETECTION AS A FUNCTION OF SECTOR LENGTH 17
   B. MULTIPLE ARRIVAL CHANNELS 21
   C. CHANGES IN VELOCITY 23
IV. INVESTIGATION TIME 25
V. FURTHER STUDY 27
VI. CONCLUSIONS 29
BIBLIOGRAPHY 31
INITIAL DISTRIBUTION LIST 33

THIS PAGE INTENTIONALLY LEFT BLANK

LIST OF FIGURES

Figure 1. Sensor and targets location as a function of time in a B/F trajectory. 3
Figure 2. Sensor and targets location as a function of time in an LTO trajectory. 3
Figure 3. Derivative of the rate function when X~Normal R~Exponential 13
Figure 4. Derivative of the rate function when X~Normal R~Uniform.....14
Figure 5. Sensor location as a function of time for B/F trajectory.....17
Figure 6. Graphic example of C(x,u) with R~Exponential 18
Figure 7. Multiple arrival channels 21

THIS PAGE INTENTIONALLY LEFT BLANK

EXECUTIVE SUMMARY

Borders are monitored and protected by border patrol agents, video cameras, ground sensors, physical barriers, land vehicles and manned aircraft. The diverse nature of U.S. border defense is challenged by an equally diverse array of threats, ranging from terrorists to drug smugglers, arms dealers and human traffickers.

This paper presents a model for a moving sensor patrolling a perimeter. The goal is to find a patrol policy for the sensor that minimizes the infiltration across the perimeter (maximize detections). We assume the sensor follows a periodic trajectory at constant speed. The controlled parameters (decision variables) of the trajectory are the beginning and end points of the patrolled sector.

Theoretical framework is established for two general trajectories: a Back and forth (B/F) trajectory and a Leap to origin (LTO) trajectory.

The LTO trajectory represents cases where the perimeter is scanned at a constant speed (or constant angular speed in case of a stationary camera) from the origin to a certain point, and then instantaneously starts to be scanned from the origin again.

The two main assumptions in this paper are that the target arrival process is a constant rate Poisson process and the target arrival locations, arrival times and reneging times are independent. For convenience, it is assumed that the sensor's speed is 1. It is then shown that the results can be adapted for any sensor speed.

Properties of these trajectories are demonstrated in great generality. The results give decision makers a powerful tool for optimally deploying and operating a variety of sensors in an area of interest.

THIS PAGE INTENTIONALLY LEFT BLANK

I. INTRODUCTION

A. GENERAL

Borders are monitored and protected by border patrol agents, video cameras, ground sensors, physical barriers, land vehicles and manned aircraft. The diverse nature of U.S. border defense is challenged by an equally diverse array of threats, ranging from terrorists to drug smugglers, arms dealers and human traffickers. An increasingly common approach to border surveillance is to use a combination of long range sensors and short range sensors [1]. Generally, there is a tradeoff between the range of the sensor and its resolution; long range sensors provide less resolution than short range sensors [1].

Although the moving sensor model developed in this paper can be applied to a variety of monitoring systems, we focus on a UAV-mounted sensor and a scanning camera system.

There are two different types of UAVs: drones and remotely piloted vehicles (RPVs). Both are pilot-less, but drones are programmed for autonomous flight, whereas RPVs are actively flown, remotely, by a ground control operator. UAVs have played key roles in recent conflicts [2], providing reconnaissance, surveillance, target acquisition, search and rescue, battle damage assessments and attack capabilities. An example of such a system that is increasingly present in U.S. border surveillance activities is the Predator B UAV system, which can provide long-endurance surveillance and communications relay [3].

While UAVs are used to extend the surveillance range, especially in the absence of ground infrastructure, ground-based electro-optical sensors achieve greater resolution. A variety of electro-optical imaging sensors are employed in border surveillance. A few examples of the technologies in use are high-resolution imaging, motion detection, temperature-differentiation and night-vision devices. In addition there is wide use of commercially available CCTV cameras adapted for daytime surveillance, infrared video (IR) detection systems and laser illumination systems that enable high-resolution imaging. Other optical components include computer-operated pan/tilt/zoom cameras,

visible or near-infrared illuminators for night vision with conventional cameras and image-intensifiers for long-range night vision [1].

The combination of different sensors mitigates the shortcomings of each single sensor. For example, IR provides detection in atmospheric conditions where video imaging is ineffective, even though the resolution it provides is relatively low. Laser illumination sensors provide a combination of long range and high resolution images [5].

B. PREVIOUS WORK

Previous work on linear patrols mainly concerns anti-submarine warfare. The classic WWII "Search and screening" by Kooperman [7] lays the foundations for analyzing the performance of barrier patrols. In previous models of barrier patrols the sensor's range is taken into account. Washburn, [9] and [10], supports and enhances the basic barrier patrol model. More work on barrier patrol had been done specifically for Anti-Submarine Warfare. In this work the acoustic degradation of the sonar sensor caused by increasing the patroller speed is incorporated into the model, and the optimal patrol speed is found.

A game analysis of choice of speeds by infiltrator and patroller originated in Kettelle and Wagner [11], a precursor to [8], and was developed analytically for a continuum of speed choices by Langford [12].

C. THE MODEL FRAMEWORK

This paper sets forth a model for a moving sensor that patrols a perimeter. The goal is to find a patrol policy that minimizes the infiltration across the barrier (maximize detections) when the sensor follows a periodic trajectory at constant speed. The controlled parameters (decision variables) of the trajectory are the beginning and end points of the patrolled sector.

We now describe the two main components of the problem: sensor and targets

Sensors. We consider two types of sensors:

A UAV-mounted sensor that travels along a uni-dimensional perimeter, possibly of infinite length, and performs a back and forth motion with a constant speed as described in the picture below. This trajectory will be referred to as a B/F trajectory; see Figure 1.

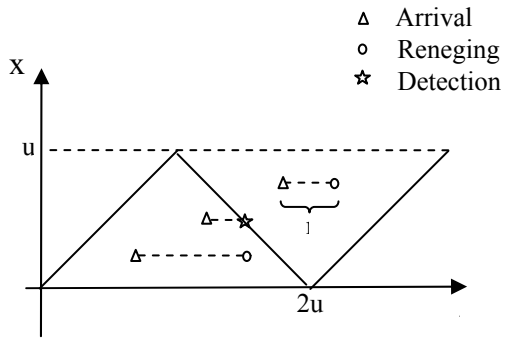

Figure 1. Sensor and targets location as a function of time in a B/F trajectory.

1. A human operated camera that scans a sector. The camera starts at the origin, moves at constant speed to a certain destination point, and then leaps to the origin instantaneously. This is referred to as a "Leap To Origin" (LTO) trajectory; see Figure 2.

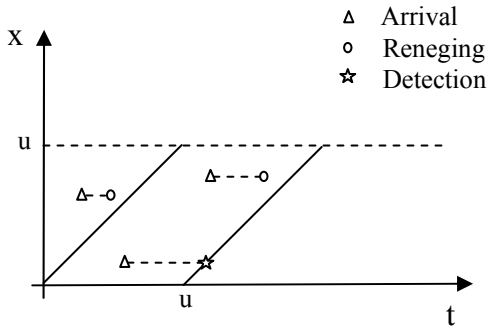

Figure 2. Sensor and targets location as a function of time in an LTO trajectory.

In both B/F and LTO we assume the origin and destination are constant in time and the speed is also constant and equals 1. Cycle time is the time it takes the sensor to depart from the origin and arrive back to the origin.

Targets: Targets arrive to the perimeter according to a Poisson process with rate $\alpha(t)$, $t \geq 0$. More specifically, let $T=(T_i : i \geq 0)$ be the collection of arrival epochs, then the number of arrivals by the time t, $t \geq 0$ is given by

$$N_a(t) = \sum_{i=1}^{\infty} I(T_i \le t), \tag{1}$$

where

$$EN_a(t) = \int_0^t \alpha(u)du\,. \tag{2}$$

The arrival location of the targets in the perimeter is described as the collection of IID rv's $X=(X_i : i \ge 0)$ defined on the same probability space as T, and are conditionally independent of arrival epochs, so that X_i may be dependent on T_i

$$P(X_i \in dx \mid T_1,...,T_i) = P(X_i \in dx \mid T_i)\,. \tag{3}$$

After a certain amount of time a target may no longer be available for detection; this can represent the fact that the target infiltrated across the perimeter successfully. We call the period of time elapsed from target arrival until infiltration the reneging time. The reneging behavior is described by a collection of IID rv's $R=(R_i : I \ge 0)$ defined on the same probability space as T. The R_i s are also conditionally independent

$$P(X_i \in dx \mid T_1,...,T_i, X_1,...,X_i) = P(X_i \in dx \mid T_i, X_i)\,. \tag{4}$$

The interpretation is that reneging behavior may be dependent on the arrival epoch and on the arrival location.

The main vehicle for our formulation is the process $N_d(t)$, that counts the number of detections by time t. The expression for $N_d(t)$ and $EN_d(t)$ depends on the trajectory policy, and will be developed in Sections Two and Three.

Examples of target behavior are shown in Figures 1 and 2. The targets' arrival times and arrival locations are marked with triangles and the reneging time intervals are marked with a broken black line. If a target reneges before the next arrival of the sensor to its location, it exits the system without being detected and the reneging time is marked with a circle. If the sensor visits the target's location before it reneges, the target is detected and the detection time is marked with a star.

This paper establishes a framework for the employment of UAV and camera-based sensor platforms; specific contributions include the following:

1. In the LTO setting, the measures of effectiveness (MOEs) are the target detection rate and the time elapsed from target arrival to its detection (waiting time). We obtain the optimal trajectory length and its location under general conditions. This is the subject of Section One.

2. In the B/F setting, the measure of effectiveness (MOEs) is the target detection rate. We obtain the optimal trajectory lengths and location, and compare the B/F and LTO performance. This is the subject of Section Three.

3. We study the case where detection is not instantaneous and each target is inspected by the sensor for a certain amount of time.

THIS PAGE INTENTIONALLY LEFT BLANK

II. THE LTO TRAJECTORY

A. THE RATE OF DETECTION AS A FUNCTION OF SECTOR LENGTH

Our goal is to find the scanning policy that maximizes the expected detection rate, prior to reneging, per-cycle. It is assumed that the sensor always travels with a constant speed. For simplicity, the sensor speed in the following formulations is 1. In Section Three, we discuss the case where the sensor has a different speed than 1. We study the simplest possible case, where T, X and R are independent and independent of the arrival process, which is a homogenous Poisson process with rate 1. Additionally, we assume that $F_x(\cdot)$ is continuously differentiable, and $F_R(\cdot)$ is continuous on (0,∞), where $F_x(\cdot)$ is the CDF of X, and $F_R(\cdot)$ is the CDF of R.

This assumption guarantees that $F_x(\cdot)$ is sufficiently smooth for our optimization problems, and is satisfied by any rv with a continuous density function. Let

$$h(u) := \sup_a \{F_x(a+u) - F_x(a)\} \quad \forall u : u \geq 0, \tag{5}$$

and $a^* = a(u)$ be the maximizer in the last equation, i.e., the best UAV origin for a cycle of length u. Clearly $h(\cdot)$ is continuously differentiable. Observe that $h(0) = 0$, $h(u) \to 1$ as $u \to \infty$ and $h(u)$ is non-decreasing. Therefore, $h(\cdot)$ is a distribution function with domain [0, ∞); in particular, $h(\cdot)$ has a continuous density $h'(\cdot)$.

Example 1. When $X \sim N(0, \sigma^2)$ we get

$$h(u) = \Phi(u/2\sigma) - \Phi(-u/2\sigma) = 1 - 2\Phi(-u/2\sigma), \tag{6}$$

where $\Phi()$ is the distribution function of a N(0,1) rv, and $a^* = -u/2$.

For a sensor with origin a^* and destination a^*+u, we have

$$N_d((k+1)u) = N_d(ku) + \sum_{i=1}^{\infty} I(a^* \le X_i \le a^*+u, X_i + (k-1)u \le T_i \le X_i + ku, R_i > X_i + ku - T_i) \tag{7}$$

for $k \ge 1$ is the number of detections at the end of the (k+1)'th cycle, and

$$N_d(u) = \sum_{i=1}^{\infty} I(a^* \le X_i \le a^*+u, T_i \le X_i, R_i > X_i - T_i) \tag{8}$$

is the number of detections at the end of the first cycle. Proposition 4.4.1 of [6] implies that, along a location $X = x$ arbitrary, the number of detections in cycle $k, k \ge 2$, of length u is a non-homogenous Poisson process with instantaneous rate $P(R > t), 0 < t \le u$.

Using Proposition 4.4.1 of [6] once more to account for the randomness in arrival locations, the expected number of detections per cycle of length u is

$$E\left(N_d((k+1)u) - N_d(ku)\right) = h(u)\int_0^u \overline{F}_R(t)dt\,, \tag{9}$$

where $\overline{F}_R(\cdot) = 1 - F_R(\cdot)$, Therefore, the expected detection rate prior to reneging is

$$g(u) := h(u)\frac{\int_0^u \overline{F}_R(t)dt}{u}\,. \tag{10}$$

The fact that $u = EN_a(u)$ leads to a second interpretation of Equation (5): $g(u)$ is the ratio of the expected number of detections by time u and the expected number of arrivals by time u. Accordingly, our goal in the LTO setting is to find a cycle length u^* that maximizes $g(.)$.

Remark: Changing the arrival rate of the Poisson process changes $g(.)$ by a constant factor, but does not change u^*.

We define $g(0) = 0$. To complete the notation, let $\bar{r} := \inf\{v : F_R(v) = 1\}$, and $\bar{u} := \inf\{v : h(v) = 1\}$; both $\bar{r}$ and $\bar{u}$ can possibly be infinite.

The following examples illustrate the scenario; we start by analyzing the case when the mass of R is concentrated in a finite time interval.

Example 2. Suppose that $0 < \bar{r} < \infty$, so that R has no mass to the right of $\bar{r}$. Then Equation (5) becomes

$$g(u) = \begin{cases} h(u)\dfrac{\int_0^u \overline{F}_R(t)dt}{u} & \text{for } 0 \le u < \bar{r} \\ h(u)\dfrac{ER}{u} & \text{for } u \ge \bar{r} \end{cases} . \qquad (11)$$

When is it optimal to stop scanning before the cycle length reaches $\bar{r}$? The following lemma addresses this question.

Lemma 1. Suppose $0 < \bar{r} < \infty$ and that $uh'(u) < h(u)$ for $u \ge \bar{r}$. Then $u^* \le \bar{r}$.

Proof outline. It is sufficient to show that $\bar{r} = \arg\max_{u \ge \bar{r}} h(u)/u$. Observe that $h(u)/u \to 0$ as $u \to \infty$, and that $h(\bar{r})/\bar{r} > 0$. Now $uh'(u) < h(u)$ for $u \ge \bar{r}$ implies $(h(u)/u)' < 0$ in $(\bar{r}, \infty)$, so that there is no stationary point in $(\bar{r}, \infty)$.

The borderline case is $uh'(u) = h(u)$ for $u \geq \bar{r}$, and we must have $h'(u)$ constant (i.e., uniform) on $u \geq \bar{r}$; see Example 3 below.

Under the conditions of Lemma 1 it is never beneficial to patrol a sector longer than $\bar{r}$ because the detections gained by covering more area will not out-weight the extra missed detections due to reneging.

Two special cases of Lemma 1 are presented.

Example 2.a) R is deterministic, i.e., $P(R = \bar{r}) = 1$ for some constant $\bar{r} > 0$. Equation (10) becomes

$$g(u) = \begin{cases} h(u) & for\ 0 \leq u < \bar{r} \\ h(u)\dfrac{\bar{r}}{u} & for\ u \geq \bar{r} \end{cases} . \tag{12}$$

Because $g(.)$ is non-decreasing on $0 \leq u \leq \bar{r}$, we have $u^* = \arg\max_{u \geq \bar{r}} \{h(u)/u\}$. If $h(.)$ meets the assumptions of Lemma 1, then $u^* = \bar{r}$.

Example 2.b) If $R \sim U(0, \bar{r})$, Equation (10) becomes

$$g(u) = \begin{cases} h(u)\left(1 - \dfrac{u}{2\bar{r}}\right) & for\ 0 \leq u < \bar{r} \\ h(u)\dfrac{\bar{r}}{2u} & for\ u \geq \bar{r} \end{cases} . \tag{13}$$

The last example can also be interpreted in terms of average waiting time. More precisely, suppose we wish to find the optimal cycle length in order to minimize the targets' average waiting time. By time $t > u$, total waiting time is given by

$$\bar{h}(u)\ \frac{t^2}{2}\ + h(u)\ \frac{t}{u}\ \frac{u^2}{2}\ . \qquad (14)$$

expected waiting time of customers that fall outside the sensor's sweeping region

number of cycles by time t

expected waiting time per cycle

It is easy to see that minimizing the last expression is akin to maximizing $h(u)(t-u)$, which is the top branch in the RHS of Equation (11). The next lemma addresses this scenario, but first some notation must be introduced: Suppose that $x(t), y(t)$ are real functions, we say that $x(t) \sim y(t)$ if $\lim_{t\to\infty} x(t)/y(t) = 1$.

Lemma 2. Assume that h(.) is strictly concave. Then $u^*(t) = \arg\max_{u<t} h(u)(t-u)$ is unique. Moreover, if $\log\left(h'(u)\right) \sim -I(u)$, for $I(.)$ a strictly increasing function such that $\liminf I(u)/u^{\kappa} \geq 1, \kappa > 0$, then $u^*(t) \sim I^{-1}\left(\log(t)\right)$.

Proof outline. For $h(u)$ strictly concave on (0,t) implies $h(u)(t-u)$ strictly concave. Additionally, $\left(h(u)(t-u)\right)' > 0$ for all $u \in (0, \varepsilon(t))$ and $\left(h(u)(t-u)\right)' < 0$ for all $u > \xi(t)$. Because $\left(h(u)(t-u)\right)'$ is continuous and strictly decreasing, we must have $\left(h(u^*(t))(t-u^*(t))\right)' = 0$ for some $u^*(t) \in \left(\varepsilon(t), \xi(t)\right)$, and $u^*(t)$ unique. For the last part, $\left(h(u)(t-u)\right)' = 0$ iff $\log h(u) - \log(1-u/t) = \log t + \log\left(h'(u)\right)$. An expansion in series now yields the result.

The last lemma says that if the density $h'(.)$ decays exponentially fast with rate $I(.)$ (which is the case for most densities of practical interest), then the optimal cycle length (in terms of waiting time) grows in time like $I^{-1}(\log(t))$.

Example 1 (continued). In the setting of Example 1, we get $h'(u) = \phi(-u/2)/\sigma$, so that $I(u) = (u/2\sigma)^2$ and $u^*(t) \sim 2\sigma\sqrt{\log(t)}$.

Our next lemma considers the case of $\bar{u}$ finite.

Lemma 3. Suppose that $0 < \bar{u} < \infty$. Then $u^* \leq \bar{u}$.

Proof outline. The fact that $\int_0^u \overline{F}_R(t)dt/u$ is non-increasing in u, and that $h(u)=1$ for all $u \geq \overline{u}$, implies that $u^* \leq \overline{u}$.

Lemma 3 is the scenario corresponding to the rv X taking values in some bounded set. It says that it is not beneficial to patrol further than $\overline{u}$, where there are no targets arriving.

Example 3. Suppose $X \sim U[0,\overline{u}]$, then Equation (1) is

$$g(u)=\begin{cases}\dfrac{\int_0^u \overline{F}_R(t)dt}{\overline{u}}, & \text{for } 0 \leq u \leq \overline{u} \\ \dfrac{\int_0^u \overline{F}_R(t)dt}{u}, & \text{for } u > \overline{u}\end{cases}. \tag{15}$$

Clearly, $u^*=\overline{u}$. In particular, if $\overline{r} < \overline{u}$, any $u^* \in [\overline{r},\overline{u}]$ is optimal.

B. OPTIMALITY CONDITIONS

We now discuss sufficient conditions for optimality in a general LTO setting. Let

$$v(u) := \frac{h'(u)}{h(u)} + \frac{\overline{F}_R(u)}{\int_0^u \overline{F}_R(t)dt} - \frac{1}{u}, \tag{16}$$

and observe that $v(.)$ is continuous on $(0,\infty)$. Setting $g'(u)=0$ in Equation (1) and rearranging yields $v(u)=0$. We are interested in finding conditions that guarantee that there exists a unique point u^* such that $v(u^*)=0$, which then would imply that u^* is the best cycle length (because $u^*=0$ is not optimal, and $g(u) \to 0$). Clearly, $v(u)>0$ for all

$u \in (0, \varepsilon), \varepsilon > 0$, and observe that $\limsup v(u) < 0$. Now the continuity of $v(u)$ ensures that u^* is unique if $v'(u) < 0$. We summarize this discussion in the next lemma.

Lemma 4. If $v'(u) < 0$ for all $u > 0$, then there exists a unique finite u^* that maximizes $g(.)$ (and is the root of $v(u^*) = 0$).

Lemma 4 says that we increase cycle length until the point where the marginal increase in target detections equals the marginal decrease in lost target detections due to reneging.

Remark. Dropping the condition $v'(u) < 0$ raises the possibility of having more than one stationary point, in which case we need to compare all the roots of $v(.)$.

As an application of the last lemma, we have the following examples.

Example 4. Suppose $X \sim N(0,1)$ and $R \sim \exp(1)$, then Equation (13) yields $u^* =$ 2.0481; see Figure 3.

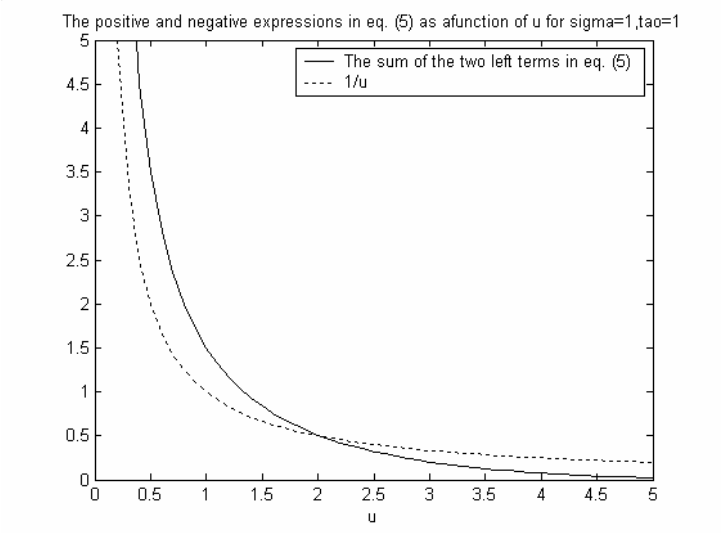

Figure 3. Derivative of the rate function when X~Normal R~Exponential

The reneging distribution being exponentially distributed leads to the same solution that arises in the following setting: Upon arrival, each target emits a signal of constant amplitude that decays exponentially in time with rate θ; this is known as a shot

noise process ([6], p.326). In particular, the signal strength of arrivals detected in the (k+1)'th cycle is given by

$$\sum_{i=1}^{\infty} e^{-\theta(X_i+ku-T_i)} I(a^* \le X_i \le a^* + u, X_i + (k-1)u \le T_i \le X_i + ku). \qquad (17)$$

Following the approach taken in [6], p. 326, we find the expected average signal strength of targets detected in an arbitrary cycle is $h(u)\int_0^u e^{-\theta t} dt / u$, which is $g(u)$ when $R \sim \exp(\theta)$. In other words, a system where targets that arrive according to a shot noise process, have the same solution as the system where targets renege according to an exponential distribution.

Example 5. Let $X \sim N(0,1)$ and $R \sim U(0,2)$. Equation (13) yields u^*=1.8626; see Figure 4 below.

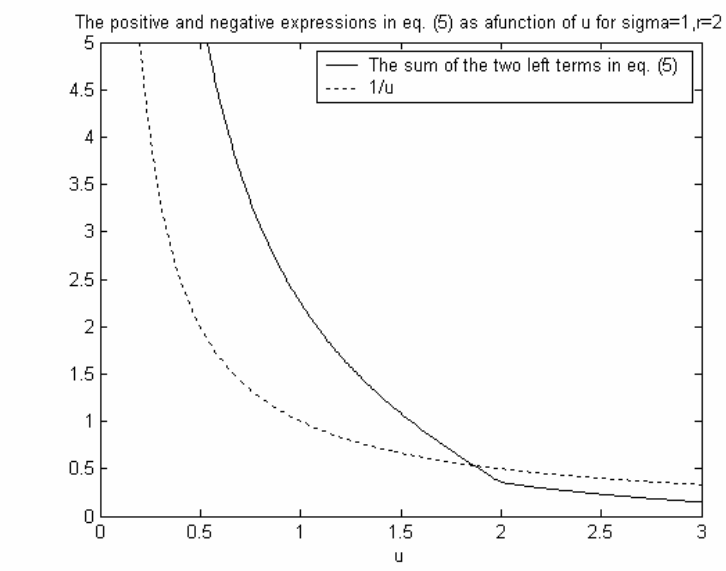

Figure 4. Derivative of the rate function when X~Normal R~Uniform

C. CHANGES IN VELOCITY

A change in the sensor's velocity from 1 to $v > 0$ changes Equation 1 to $g_v(u) := h(u)\int_0^{u/v} \overline{F}_R(t)dt/(u/v)$. Changing variables, the latter equals $h_v(u')\int_0^{u'} \overline{F}_R(t)dt/u'$, where $h_v(u') := h(u'v)$. Because for $v > 0$ arbitrary, $h_v(u')$ is a distribution, the analysis of this section applies to the general velocity setting, with $h_v(.)$ in place of $h(.)$. It can easily be seen that $u_v^* \le u^*$ and $g_v(u_v^*) \le g(u^*)$ if and only if $v \le 1$; in other words, decreasing the velocity reduces the optimal cycle length and the optimal detection rate.

D. SCANNING OF DISJOINT SECTORS

Our definition of h(.) (cf. Equation (1)) constrains the camera operator to scan a continuous sector. In reality, however, there may exist sectors that are impassable, in which case the camera operator skips the forbidden sector to scan a more promising area. From the theoretical standpoint, this scenario is captured by letting the rv X have a multimodal density function, and by relaxing our definition of h(.). Given n, a positive integer, let $W^n := \bigcup_{i=1}^{n}[a_i, b_i), a_1 \le b_1 \le a_2 \le b_2 \le \mathrm{L}\ \le a_n \le b_n$, and define

$$\hat{h}(u) := \max_{a_1 \le b_1 \le a_2 \le b_2 \le \mathrm{L}\ \le a_n \le b_n} \left\{ \int_{x \in W^n} f_X(x)dx : \sum_{i=1}^{n}(b_i - a_i) = u \right\}. \tag{18}$$

The constant n represents the number of disjoint sectors that the operator may scan before going back to the origin. Clearly, for $a_2 = b_2, ..., a_n = b_n$, we end up with Equation (1) and, moreover, all our developments in this section remain valid with $\hat{h}(.)$ in lieu of $h(.)$. The fact that $\hat{h}(.)$ is concave (as can be seen by evaluating $\hat{h}''(.)$), implies that $u\hat{h}'(u) < \hat{h}(u)$ for all $u \ge 0$, and so strengthens Lemma 1.

Corollary 5: Suppose $0 < \overline{r} < \infty$. Then $u^* \le \overline{r}$.

THIS PAGE INTENTIONALLY LEFT BLANK

III. THE BACK AND FORTH TRAJECTORY

A. RATE OF DETECTION AS A FUNCTION OF SECTOR LENGTH

The back and forth trajectory scenario arises for platform mounted sensors, such as UAVs and manned aircraft. In this section our goal is to analyze cycle trajectories and find an optimal cycle length, where optimal means "maximum expected detection rate prior to reneging." A typical trajectory, with speed 1, is illustrated in Figure 5.

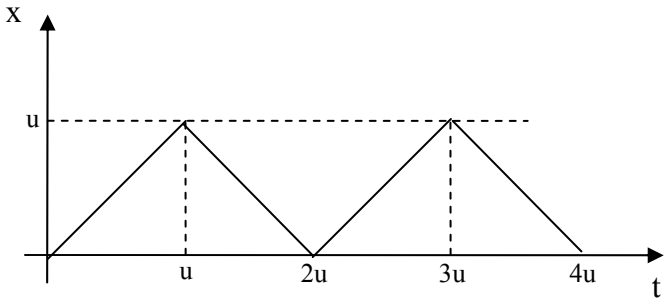

Figure 5. Sensor location as a function of time for B/F trajectory

Our setting is the same as for the LTO scenario: $X, R,$ and $N_a(t)$ are mutually independent for all $t > 0$, the speed of the sensor is 1; and the arrival process is Poisson with rate 1. With these simplifying assumptions, Figure 5 indicates that because the sensor visits the trajectory edges one-half as frequently as the trajectory center, targets will renege more often in the edges of the trajectory. Following a similar approach as the one used to reach Equation (1), it can be seen that the expected detection rate prior to reneging is given by

$$g(u) := \frac{\sup_{\delta} \left\{ \int_0^u f_X(x+\delta) c(x,u) dx \right\}}{2u}, \tag{19}$$

where

$$c(x,u) := \int_0^{2x} \overline{F}_R(t)dt + \int_0^{2(u-x)} \overline{F}_R(t)dt,\ 0 \le x \le u\ . \tag{20}$$

The constant $x^*_0 = x^*(u)$ associated with the supremum in Equation (19) is the trajectory origin that maximizes the correlation between $c(.,u)$ and the arrival location density $f_X(.)$. Regarding the function $c(.,.)$, it can easily be seen that it is symmetric in its first argument around $x = u/2$ and, taking second partial derivatives with respect to x, it is concave non-increasing in x. Figure 6 illustrates $c(.,.)$ for the exponential reneging case.

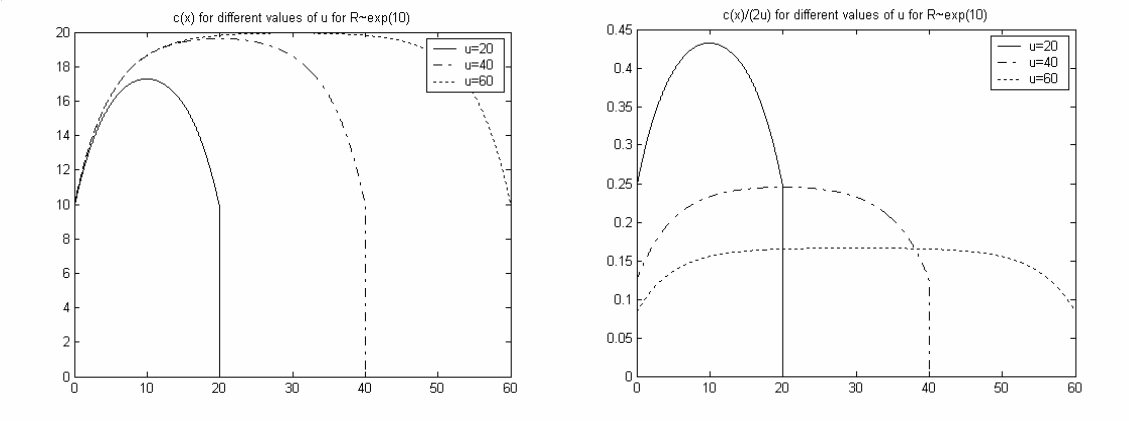

Figure 6. Graphic example of C(x,u) with R~Exponential

The additional reneging present in the B/F trajectory suggests that this policy can do no better than LTO; this is made precise in the next lemma.

Lemma 5. For all $u \ge 0$, $g_{BF}(u) \le g(u)$.

Proof outline. The result follows because $\overline{F}_R(.)$ non-increasing implies that $c(x,u) \le 2\int_0^u \overline{F}_R(t)dt$, for all $0 \le x \le u$.

We now focus on finding an optimal cycle length $u^*_0 = \arg\max g_{BF}(u)$. The analogue of Lemma 3 to the B/F setting is straightforward.

Lemma 6. Suppose $P(\underline{u} \le X \le \overline{u}) = 1$, where $\underline{u} = \sup\{u : P(X \ge u) = 1\}$ and $\overline{u} = \inf\{u : P(X \le u) = 1\}$, and $-\infty < \underline{u} < \overline{u} < \infty$. Then $\theta \le \overline{u} - \underline{u}$.

Proof outline. For $u_+ \ge \overline{u}$ and $u_- \le \underline{u}$, we have

$$\frac{\int_{u_-}^{u_+} f_X(x)c(x,u)dx}{2(u_+ - u_-)} = \frac{\int_{\underline{u}}^{\overline{u}} f_X(x)c(x,u)dx}{2(u_+ - u_-)} \le \frac{\int_{\underline{u}}^{\overline{u}} f_X(x)c(x,u)dx}{2(\overline{u} - \underline{u})}. \qquad (21)$$

The other possibilities ($u_- > \underline{u}, u_+ > \overline{u}, u_+ - u_- > \overline{u} - \underline{u}$; $u_- < \underline{u}, u_+ < \overline{u}, u_+ - u_- > \overline{u} - \underline{u}$) are treated similarly.

Lemma 7 is the equivalent of Lemma 1.

Lemma 7. Suppose that $0 < \overline{r} < \infty$, and that

$$\left(f_X(u + \theta) - \eta'(u, \overline{r})\right)u \le F_X(u + \theta) - F_X(\theta) - \eta(u, \overline{r}), \qquad (22)$$

for all $u \ge \overline{r}$. Then $\theta \le \overline{r}$.

Remark. The last condition is the same as the condition used in Lemma 1, except for the error term

$$\eta(u, \overline{r}) := \frac{\int_0^{\overline{r}/2} f_X(x + \theta)\left(ER - \int_0^{2x} \overline{F}_R(t)dt\right) + \int_u^{u-\overline{r}/2} f_X(x + \theta)\left(ER - \int_0^{2(u-x)} \overline{F}_R(t)dt\right)}{2ER}. \qquad (23)$$

The error term becomes insignificant as $\overline{r}$ becomes large, but may be relevant for small values of $\overline{r}$; see Example 6 below.

Proof outline. For $u \geq \bar{r}$ we have

$$g'(u) = ER\frac{F_X(u+\delta^*) - F_X(\delta^*) - \eta(u,\bar{r})}{u}, \tag{24}$$

and the hypothesis implies that $g'(u) < 0$ for all $u \geq \bar{r}$.

Example 6. When $P(R = \bar{r}) = 1$ for some constant $\bar{r} > 0$

$$c(x,u) = \min\{(2x), \bar{r}\} + \min\{2(u-x), \bar{r}\}. \tag{25}$$

Clearly, $g(u) = F_X(u+\delta^*) - F_X(\delta^*)$ is non-decreasing for $u \leq \bar{r}/2$. Therefore, if the conditions of Lemma 7 apply, $\bar{r}/2 \leq \delta^* \leq \bar{r}$. Once again, the extra reneges that may occur at the tails of the B/F trajectory, when compared with LTO, produce $\delta^* \leq u^*$.

Regarding the general case when both X and R have infinite support, let

$$v(u) := \frac{f(u+\delta^*)\int_0^{2u} \bar{F}_R(t)dt}{\int_0^u f(x+\delta^*)c(x,u)dx} - \frac{1}{u}. \tag{26}$$

Lemma 8. If $v'(u) < 0$ for all $u > 0$, then there exists a unique finite u^* that maximizes $g(.)$ (and is the root of $v(u^*) = 0$).

Proof outline: The proof follows along the lines of the proof of Lemma 4, once we notice that $g'(u) = 0$ iff $v(u) = 0$..

B. MULTIPLE ARRIVAL CHANNELS

It is often the case that one UAV is available in a sector of interest with more than one concentration of target arrivals. The problem in this case is deciding how many and which of these concentrations (referred to here as "channels of arrival") to patrol in order to maximize the overall detection rate. When the channels of arrival are narrow compared to the distances between them, they can be approximated by channels of width zero. This approximation is valid in various scenarios, such as targets that travel along roads or narrow valleys. The main issue in this case is the tradeoff between covering more areas of interest and missing detections by "wasting" additional time to travel between the channels.

We will show that this problem can be written as a nonlinear integer programming problem. In addition to enabling the solution of the problem by enumeration, the formulation provides some insight about these types of problems.

More specifically, we discuss the case of a sector with n channels of arrival, which are all zero in width. We still maintain the assumption that the overall arrival rate is 1. The pdf of the arrival locations is defined as $P(\textit{arrival in channel } i) := p_i : \sum_{i=1}^{n} P_i = 1$.

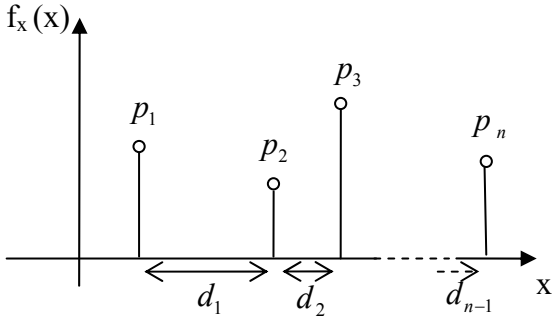

Figure 7. Multiple arrival channels

Let $d_i : i = 1..n-1$ be the distances between the channels, where d_i is the distance between channel i and channel $i+1$.

The patrolled sector length when patrolling from channel k to channel $l : l \geq k$ and back is

$$u_{k,l} = \begin{cases} 0 & l = k \\ \sum_{i=k}^{l-1} d_i & l > k \end{cases}, \tag{27}$$

which is also the distance between channels k and l.

Consequently, the overall detection rate given k and l is

$$\tilde{g}(k,l) = \frac{1}{2u_{k,l}} \sum_{j=k}^{l} p_j c(u_{k,j}, u_{k,l}) . \tag{28}$$

The problem of deciding which channels to patrol in order to maximize the overall detection rate could be written as

$$\max_{k,l} \left\{ \frac{1}{2u_{k,l}} \sum_{j=k}^{l} p_j c(u_{k,j}, u_{k,l}) \right\} : 1 \leq k \leq l \leq n . \tag{29}$$

The inputs to this nonlinear integer programming problem are:

1. The distances between the channels of arrival
2. The probability of arrival at each channel
3. The reneging time distribution (needed to calculate $c(u_{k,j}, u_{k,l})$).

Example 7. In the instance of the aforementioned case, targets are expected to arrive at one of two roads with identical probability, $p = 1/2$ .The distance between the roads is d. The dilemma in this case is to choose between surveying one road constantly and moving back and forth between the two roads.

In our case, the detection rate can be written as a function of the number of channels patrolled $m = 1,2$

$$\widetilde{g}(m) = \begin{cases} p & m = 1 \\ \int_0^{2d} \overline{F}_R(t)dt & \\ 2p\dfrac{0}{2d} & m = 2 \end{cases} . \tag{30}$$

The above result is very useful in producing a quantitative decision rule. By this rule it is beneficial to patrol both roads only if

$$\frac{\int_0^{2d} \overline{F}_R(t)dt}{2d} > 1/2 . \tag{31}$$

The interpretation of the above condition is that when the probability of missing a target due to traveling between the roads is greater than ½, it is better to survey only one road.

Furthermore, if the reneging time is always shorter that the round trip between the two roads, $\bar{r} < 2d$, this condition becomes $ER > d$.

C. CHANGES IN VELOCITY

We approach the investigation of the effect of the sensor speed in a similar way to the LTO case (section 3.3). A change in the sensor's velocity from 1 to $v > 0$ changes Equation (19) to:

$$\widetilde{g}_v(u) = \frac{\sup_a \left\{ \int_0^u f_X(x+a)c(x/v, u/v)dx \right\}}{2u/v} . \tag{32}$$

Changing variables, the latter equals:

$$\frac{\sup_{a'}\left\{\int_0^{u'} f_X^v(x'+a')c(x',u')dx'\right\}}{2u'}, \tag{33}$$

where $f_X^v(x') := vf_X(x'v)$. Because for $v>0$ arbitrary, $f_X^v(x')$ is a density function, the analysis of this section applies to the general velocity setting, with $f_X^v(.)$ in place of $f_X(.)$. It is also evident that $u_v^* \le u^*$ and $g_v(u_v^*) \le g(u^*)$ if and only if $v \le 1$. The meaning is that, just as for the LTO trajectory, decreasing the velocity reduces the optimal cycle length and the optimal detection rate.

IV. INVESTIGATION TIME

So far we made the assumption that the trajectory of the sensor is predetermined and does not change due to real time events. In certain situations, however, targets are investigated by the sensor upon detection, during which time the sensor remains immobile. This type of sensor policy is common when the identification of the target is required before a decision is made as to the necessary reaction, or when the sensor has to "escort" the target until the reaction force arrives at the scene. In these cases, a dynamic real time algorithm is needed in order to maximize the MOE.

Specifically, suppose that each target is investigated κ units of time after detection, and that $\eta(x,t)$ represents the clock when position x was last visited. In the LTO setting, we assume that at any instant the camera operator has the option of continuing to move rightward, or it can make an instantaneous leap to any leftward point. Our MOE is "expected time until the first detection," and we wish to select a leftward leaping point or continue moving rightward in order to minimize that MOE. In the B/F framework there are only two options: move towards the left or to the right, so the analysis is somewhat simpler. In either case, we make the same basic assumptions: the rv's X and R are independent, and independent of the arrival process, which is homogeneous Poisson; we also assume that sensor velocity is 1. Clearly the setup is markovian, in that future detections depend only on the current sensor position and on the latest visiting times to each location in the perimeter. Let $\pi(t_0)$ be the sensor's position at time t_0, and suppose the sensor does not change course (leap in LTO or change course in B/F). Then

$$P(\text{no detections in next } \Delta\text{t units of time}) = \int_0^{\Delta t} f(\pi(t_0)+x)\exp\left(-\int_0^{t_0+x-\eta(\pi(t_0)+x)} \bar{F}_R(z)dz\right)dx,$$

which follows because for each position x, the detection process is Poisson with rate $\bar{F}_R(t), 0<t<\eta(x)$ (cf. the discussion preceding Equation (2)), and velocity is 1. The last expression can be used to compute the expected time until the first detection without changing course, $D_{\text{no change}}(\pi,\eta)$, given position π, last visiting clock η

$$
\begin{aligned}
D_{\text{no change}}(\pi,\eta) &= \int_0^\infty P(\text{first detection occurs after t})dt \\
&= \int_0^\infty P(\text{no detection until t})dt \\
&= \int_0^\infty \int_0^t f(\pi(t_0)+x)\exp\left(-\int_0^{t_0+x-\eta(\pi(t_0)+x)} \overline{F}_R(z)dz\right)dxdt
\end{aligned}
\qquad . \qquad (34)
$$

V. FURTHER STUDY

The cases studied in this paper assume that the target arrival process is a homogenous Poisson process, and that reneging times and arrival locations are independent of each other and of the Poisson process. An important case is when the reneging times are dependent on the targets' arrival locations. Such target behavior can occur when varying terrain conditions in different locations along the patrolled perimeter affect the crossing times of the targets. As explained in the Introduction, the detection process remains Poisson under conditional independence, so that the approach taken in this paper to find optimal cycle lengths remains valid. Further work is required to explore a dependence structure that keeps our formulation analytically tractable.

An important class of scenarios arises when multiple sensors can be used in a sector. Analysis of this case boils down to the derivation of optimal employment of more than one sensor, the system's performance, the cost structure, and sensitivity to the number of sensors. Equivalently, there may exist multiple target types, with a reward associated with each type; the goal here would be to maximize the reward earning rate.

Regarding the target arrival process, arrivals in different time periods may be correlated, which destroys the Poisson assumption. A more realistic model would allow for these dependencies, also possibly taking into account spatial effects. Markov random fields, whose theory is well developed, seems the ideal candidate to explore this venue.

In our analysis it is assumed that the sensor's location does not affect the targets behavior; this assumption can be made for hidden sensors like hidden cameras and high altitude UAV's, but might not always hold. This suggests a game-theoretic facet to our problem. Specifically, targets may be smart and behave in order to lessen the probability of capture.

THIS PAGE INTENTIONALLY LEFT BLANK

VI. CONCLUSIONS

This paper presents a model for a moving sensor patrolling a perimeter. The goal is to find a patrol policy for the sensor that minimizes the infiltration across the perimeter (maximize detections). We assume the sensor follows a periodic trajectory at constant speed. The controlled parameters (decision variables) of the trajectory are the beginning and end points of the patrolled sector.

Theoretical framework is established for two general trajectories: a Back and forth (B/F) trajectory and a Leap to origin (LTO) trajectory.

The LTO trajectory represents cases where the perimeter is scanned in a constant speed (or constant angular speed in the case of a stationary camera) from the origin to a certain point, and then instantaneously starts to be scanned from the origin again.

The target behavior is described extensively in the introduction. The two main assumptions in this paper are that the target arrival process is a constant-rate Poisson process and the target arrival locations, arrival times and reneging time are independent.

The assumption that the sensors speed is 1 is made for convenience. Section 3.3 discusses the adaptation of the results for general speed.

For the LTO trajectory, we derived an expression for the rate of detection given the reneging, arrival location distribution and the length of the patrolled sector (the decision variable). In Lemma 1 it is shown that it is never beneficial to patrol a sector larger than the upper bound on the reneging time distribution, if outside it the pdf of target arrival location is non-increasing.

In a case where the variability in reneging times is very low, the reneging time can be represented as deterministic and $\bar{r}$ is the optimal sector length.

An interesting private case is when the arrival location distribution is uniform and $\bar{r}$ is smaller than the width of the arrival distribution, $\bar{u}$. In this case, the loss in detection

rate due to the increase in the sensor revisit times is equal to the gain in detection rate due to the increase in covered sector for all $u \in [\bar{r}, \bar{u}]$. The result is that all the sector lengths in that interval are optimal.

We then consider a different scenario. In this scenario, targets appear on a perimeter and do not renege. This scenario is relevant to cases where a crossing malevolent agent leaves a track at the location of its infiltration (for example, tracks on a trail). The objective in these situations is to detect the tracks left by the target within the shortest possible time. The sensor platform in this case could be a motorized ground patrol or a visual scanning sensor. Example 2.b shows that maximizing detection rate in the case of uniform reneging time is equivalent to minimizing the expected time to detection of targets (waiting time) in the aforementioned scenario.

A basic limitation of the suggested model is that the sensor footprint is modeled as a one-dimensional point. This assumption is a reasonable representation of reality when the size of the sector is significantly greater than the sensor's footprint width. Another interpretation of the model is that it represents only the component of detection that is produced by the movement of the sensor. For example, a stationary sensor has a detection rate of zero in our model, while in reality this is not necessarily true.

For the B/F trajectory, we also derived an expression for the rate of detection given the reneging, arrival location distribution and the length of the patrolled sector. In this case, unlike the LTO trajectory, the probability of target detection given its arrival location along the patrolled sector is not necessarily the same for all locations. In fact it is not the same for most realistic scenarios. This fact is captured by the expression $c(x,u)$, which represents that conditioned probability: $P(\det ection \mid u, x : x \in [0,u]) = c(x,u)$. This function is determined by the sector length and the reneging distribution.

A very close relationship exists between the detection rate in the B/F trajectory and the LTO trajectory and it is analyzed in the B/F section (III) of this paper.

BIBLIOGRAPHY

[1] Zellen, Barry S., "Preventing Armageddon I: Enhancing America's Border & Port Security After 9/11," *Strategic Insights*, Vol. III, Iss. 11, Nov 2004.

[2] Bolkcom, Christopher, "Homeland Security: Unmanned Aerial Vehicles and Border Surveillance," *CRS Report for Congress*, Jun 28, 2004.

[3] "Predator-B UAV to Patrol U.S. Borders," *General Atomics Aeronautical Systems*, Oct 3, 2005.

[4] Hall, Mirri, "Despite New Technology, Border Patrol Overwhelmed," *USA Today*, Oct 18, 2005.

[5] Interview between Haim Rousso, Co-managing Director, El-Op Electro-Optics Industries, Ltd., and the author.

[6] Resnick, Sidney, *Adventures in Stochastic Processes*, Boston, MA: Birkhäuser Boston, Inc., 1992.

[7] Koperman, Bernard O., "Search and Screening," *Operations Evaluation Group Report 56*, Washington D.C.: Office of the Chief of Naval Operations, 1946.

[8] Loane, Edward P. and Wagner, Daniel H., "Submarine-versus-Submarine Secure Sweep Width Manual," *Associates Report to Bureau of Ships*, Commander Submarine Group Two and David Taylor Model Basin, Dec 17, 1964.

[9] Washburn, Alan R., "On Patrolling a Channel," *Naval Research Logistic Quarterly*, 29 Dec 1982.

[10] Washburn, Alan R., *Patrolling a Channel Revisited*, Naval Postgraduate School, Monterey, CA.

[11] Kettelle, John D. and Wagner, Daniel H., *Acoustic Effectiveness of Specific Nuclear Submarines*, David Taylor Model Basin, Mar 31, 1963.

[12] Langford, Eric S., “A Continuous Submarine versus Submarine Game,” *Naval Research Logistics Quarterly*, 20, Sep 1973.

INITIAL DISTRIBUTION LIST

1. Defense Technical Information Center
   Ft. Belvoir, Virginia

2. Dudley Knox Library
   Naval Postgraduate School
   Monterey, California